

Manuscript Number:

Title: Impact of concurrent pressure and shear on MSC viability and differentiation during simulated intervertebral disk needle injection.

Article Type: Laboratory Investigation

Corresponding Author: Dr. Jean. F. Welter, MD, PhD

Corresponding Author's Institution: Case Western Reserve University

First Author: J. David Prologo, MD

Order of Authors: J. David Prologo, MD; Lori Duesler, BA; Jim A Berilla; Harihara Baskaran, PhD; Mark D Schluchter, PhD; Jean. F. Welter, MD, PhD

Abstract: Purpose: Imaging-guided mesenchymal stem cell (MSC) injection is a promising therapy for intervertebral disk (IVD) degeneration, a major cause of chronic disability, and has provided functional restoration in animal models. However, injection of MSCs into the IVD occurs against considerable backpressures, and the effects of combined shear and pressure on the MSCs during injection is unknown. We evaluated these effects in an in vitro model. Materials & Methods: MSC (2M or 4M cells/ml) were studied either before or after passing them through a needle (25 and 22 Ga, 7" spinal needles), into vials without and with backpressures (30 or 60 PSI). We solved Navier-Stokes equations to estimate peak shear forces. Cells were subject to live-dead assays, or chondrogenic aggregate cultures. Results: Peak shear stress (143-247 Pa), insufficient to cause cell death, occurred at the transition from the hub to the needle. The % dead cells remained unremarkably low at <11. At 21 days, chondrogenic differentiation was evident in all aggregate sections, but the cross-sectional area of the proteoglycan-positive fraction was lower in those from the no-injection groups (57% and 74% for the 2M and 4M cells/ml groups, respectively) compared to 100% in all other groups. Conclusion: Peak pressure and shear levels achieved during injection did not alter cell viability. All sheared groups had better differentiation than controls, which may represent a beneficial effect of needle delivery.

Suggested Reviewers: Jack W Jennings MD, PhD  
Assistant Professor, Musculoskeletal Section, Radiology, Mallinckrodt Institute of Radiolog,  
Washington University  
Jenningsj@mir.wustl.edu  
Expertise in spine intervention

John F Cardella MD  
Director of interventional radiology, Radiology, Geisinger Health System  
jfcardella@geisinger.edu  
Active in this field, has related publications

David C Madoff MD  
Chief of interventional radiolog, Radiology, Weill Cornell Medical Cente  
dcm9006@med.cornell.edu  
Performs related research





Cleveland, January 9, 2014

Editorial Office  
Journal of Vascular and Interventional Radiology  
Society of Interventional Radiology  
3975 Fair Ridge Drive  
Suite 400 North  
Fairfax, VA 22033

To whom it may concern,

I am attaching a manuscript entitled "*Impact of concurrent pressure and shear on MSC viability and differentiation during simulated intervertebral disk needle injection*" for consideration for publication in the regular issue of *Journal of Vascular and Interventional Radiology*.

My co-authors and myself do not have any financial conflict of interest to declare. The study was funded in part by funds from the NIH. Merrit Medical donated or lent some of the equipment used, however they were not involved in the study design or interpretation.

Please let me know if I can supply any additional information. As corresponding author, I can be reached using the contact information on this page.

With kind regards,

A handwritten signature in black ink, appearing to read "J. Welter".

Jean Welter

1  
2  
3  
4  
5  
6  
7  
8  
9  
10  
11  
12  
13  
14  
15  
16  
17  
18  
19  
20  
21  
22  
23  
24  
25  
26  
27  
28  
29  
30  
31  
32  
33  
34  
35  
36  
37  
38  
39  
40  
41  
42  
43  
44  
45  
46  
47  
48  
49  
50  
51  
52  
53  
54  
55  
56  
57  
58  
59  
60  
61  
62  
63  
64  
65

# Impact of concurrent pressure and shear on MSC viability and differentiation during simulated intervertebral disk needle injection.

---

<sup>1</sup>J. David Prologo, MD, <sup>2</sup>Lori Duesler, BA, <sup>3</sup>Jim A. Berilla, <sup>4</sup>Harihara Baskaran, PhD,  
<sup>5</sup>Mark Schluchter, PhD, and <sup>1,2</sup>Jean F. Welter, MD, PhD

<sup>1</sup>National Center for Regenerative Medicine and the Departments of <sup>2</sup>Biology, <sup>3</sup>Civil Engineering, <sup>4</sup>Chemical Engineering, and <sup>5</sup>Epidemiology & Biostatistics, Case Western Reserve University, Cleveland, OH 44106

The authors do not have any financial or other conflicts of interest to disclose.

## Acknowledgements

We thank Merit Medical for the loan of the electronics and the gift of the syringes and needles. Research reported in this publication was supported in part by the National Institute of Arthritis and Musculoskeletal and Skin Diseases of the National Institutes of Health under Award Number P01-AR053622 (Bioreactor Core Facility, JFW, HB). The content is solely the responsibility of the authors and does not necessarily represent the official views of the National Institutes of Health.

## Please address correspondence to:

Jean F. Welter

Department of Biology, Skeletal Research Center

Millis Building, room 112A

2080 Adelbert Road, Cleveland, OH 44106

T. : +1(216) 368-1333, F. : +1(216) 368-4077, Email : [jean.welter@case.edu](mailto:jean.welter@case.edu)

1  
2  
3  
4 **Abstract**  
5

6  
7 Purpose: Imaging-guided mesenchymal stem cell (MSC) injection is a promising  
8  
9 therapy for intervertebral disk (IVD) degeneration, a major cause of chronic disability,  
10  
11 and has provided functional restoration in animal models. However, injection of MSCs  
12  
13 into the IVD occurs against considerable backpressures, and the effects of combined  
14  
15 shear and pressure on the MSCs during injection is unknown. We evaluated these  
16  
17 effects in an in vitro model. Materials & Methods: MSC (2M or 4M cells/ml) were studied  
18  
19 either before or after passing them through a needle (25 and 22 Ga, 7" spinal needles),  
20  
21 into vials without and with backpressures (30 or 60 PSI). We solved Navier-Stokes  
22  
23 equations to estimate peak shear forces. Cells were subject to live-dead assays, or  
24  
25 chondrogenic aggregate cultures. Results: Peak shear stress (143-247 Pa), insufficient  
26  
27 to cause cell death, occurred at the transition from the hub to the needle. The % dead  
28  
29 cells remained unremarkably low at <11. At 21 days, chondrogenic differentiation was  
30  
31 evident in all aggregate sections, but the cross-sectional area of the proteoglycan-  
32  
33 positive fraction was lower in those from the no-injection groups (57% and 74% for the  
34  
35 2M and 4M cells/ml groups, respectively) compared to 100% in all other groups.  
36  
37 Conclusion: Peak pressure and shear levels achieved during injection did not alter cell  
38  
39 viability. All sheared groups had better differentiation than controls, which may  
40  
41 represent a beneficial effect of needle delivery.  
42  
43  
44  
45  
46  
47  
48  
49  
50  
51  
52  
53  
54  
55  
56  
57  
58  
59  
60  
61  
62  
63  
64  
65

## Introduction

Back pain is a major public health issue affecting up to a third of the industrialized world population, and is strongly associated with intervertebral disk (IVD) degeneration [1].

Patients experience pain-related quality of life deterioration, loss of productivity, and psychological distress [2]. Lumbar IVD degeneration, in particular, begins early, with clear changes found in adolescence that accumulate over the life of the patient [3]. By age 50, IVD degeneration reaches a prevalence of 88%. Costs are estimated at 50 billion dollars annually in the United States and 12 billion in the United Kingdom, either through loss of wages, medical costs, or disability benefits [2, 4].

There are few effective therapies for symptomatic degenerated discs. Conservative interventions such as intradiscal electrotherapy or nucleoplasty produce inconsistent and temporary results, similar to placebo [5-7]. Spinal fusion improves back pain, however, patient satisfaction following surgical fusion is low at 65%. Fusion (and prosthetic disc replacement) reduces spinal flexibility, and overloads adjacent segments, leading to additional surgery in 30% [8, 9].

A treatment which preserved the physiological function of the IVD would be preferable, and cell-based therapy is being explored as an option. Several groups have established methods of isolating, characterizing, expanding, labeling, and delivering adult bone marrow derived mesenchymal stem cells (MSCs) to degenerated or damaged articular surfaces [10-15]. MSCs are multipotent adult stem cells with the capacity to differentiate into several tissue types, that, when implanted into the IVD, secrete ECM constituents and growth factors. The effectiveness of this technique has been demonstrated in vitro and in animals [12, 13, 16-21], using auto- [22, 23] or allo-transplantation [24]. In early

1  
2  
3  
4 work this was done through open grafting of scaffold-MSC composites [23] as  
5  
6 engineered tissue. The interventional radiology technique of fluoroscopically guided  
7  
8 percutaneous needle access to the IVD is potentially a less invasive approach to  
9  
10 delivering MSC to the IVD [22, 25].  
11  
12

13  
14 Infusion of cells through a needle or catheter is well-established, but, in general, these  
15  
16 infusions take place into a low backpressure environment such as the peripheral venous  
17  
18 circulation in blood transfusions [26]. The effects of injection against a higher pressure  
19  
20 head have been speculated on but remain unstudied. In particular, the impact of  
21  
22 combined pressure and shear on the injected cells is not known; in this study, we  
23  
24 sought to determine whether MSCs can be injected against backpressures typical of an  
25  
26 IVD NP, without adverse effects.  
27  
28  
29  
30

## 31 32 **Materials and Methods**

### 33 34 35 **Materials**

36  
37  
38 Integra spinal needles (25 Ga x 7" and 22 Ga x 7", Integra Life sciences, Salt Lake City  
39  
40 UT). Intellisystem 25 syringes were used for injection, as were the Intellisystem display  
41  
42 and printer. These devices were loans or gifts from Merit Medical Systems (South  
43  
44 Jordan, UT).  
45  
46  
47

48  
49 Cell culture medium (Dulbecco's Modified Eagle's Medium with either 4.5 g/l – DMEM-  
50  
51 HG or 1.5 g/l glucose – DMEM-LG), trypsin, L-glutamine, antibiotic/antimycotic  
52  
53 (Penicillin G, streptomycin sulfate, and amphotericin B), non-essential amino acids, and  
54  
55 sodium pyruvate, as well as the Live-dead assay kit were obtained from Invitrogen  
56  
57 (Carlsbad, CA). A lot of fetal bovine serum (FBS) was also obtained from Invitrogen,  
58  
59  
60  
61  
62  
63  
64  
65

1  
2  
3  
4 after screening as described by Lennon et al. [27]. Recombinant human transforming  
5  
6 growth factor beta -1 (TFG-β1) was from Peptotech (Rocky Hill, NJ); recombinant  
7  
8 human fibroblast growth factor-2 (FGF-2) was generously provided by the Biological  
9  
10 Resources Branch of the National Cancer Institute. ITS<sup>+</sup> Premix™ was from  
11  
12 Collaborative Biomedical Products (Collaborative Research, Bedford, MA), while  
13  
14 ascorbate-2-phosphate was from Wako (Richmond, VA). Bovine calf serum was from  
15  
16 Hyclone (Logan, UT).  
17  
18  
19  
20

21 All cell culture plasticware was from BD Biosciences (Franklin Lakes, NJ), except for the  
22  
23 polypropylene 96-well plates which were sourced from Phenix Research Products  
24  
25 (Hayward, CA). Nominally 10 ml sterile pyrogen-free borosilicate glass septum vials  
26  
27 were obtained from Allergy Labs (Oklahoma City, OK, actual volume 12.8 ml). Syringes  
28  
29 and needles were from Becton Dickinson.  
30  
31  
32  
33

### 34 **Cells and cell culture:**

35  
36  
37 Deidentified human bone marrow aspirates were obtained through our institutional  
38  
39 Hematopoietic Stem Cell Core Facility from a single healthy adult volunteer donor  
40  
41 (female, 23 y.o., Caucasian), using a procedure reviewed and approved by the  
42  
43 Institutional Review Board and after informed consent was obtained. Briefly, 10 – 15 ml  
44  
45 of bone marrow aspirate were combined with DMEM-LG with 10% FBS and centrifuged  
46  
47 at 500 × g for 5 minutes. The cell pellet was resuspended in 5 ml of DMEM-LG with  
48  
49 10% FBS, and subjected to centrifugation over a preformed Percoll gradient. After  
50  
51 centrifugation at 460 × g, the top 25% of the gradient was collected, washed with  
52  
53 serum-containing medium, and re-centrifuged at 500 × g. Cells from the resulting pellet  
54  
55  
56  
57  
58  
59 were seeded onto 10 cm diameter plates at  $1.8 \times 10^5$  nucleated cells/cm<sup>2</sup>, and  
60  
61  
62  
63  
64  
65



1  
2  
3  
4 incubated for four days. At this point, non-adherent cells were removed by replacing the  
5  
6 medium. At this and subsequent feedings, the medium was supplemented with 10 ng/ml  
7  
8 FGF-2 (complete growth medium) [15]. Subsequently, the medium was replaced every  
9  
10 third day for approximately two weeks, after which the MSCs were subcultured using  
11  
12 0.05% Trypsin EDTA [14] and re-plated in T-175 flasks at  $5 \times 10^3$  cells/cm<sup>2</sup>. At the end  
13  
14 of first passage (7 days), the MSCs were again trypsinized, counted using a  
15  
16 hemacytometer, and then resuspended at  $2 \times 10^6$  or  $4 \times 10^6$  cells per ml in complete  
17  
18 growth medium.  
19  
20  
21  
22

23  
24 For chondrogenic differentiation experiments, a defined chondrogenic medium was  
25  
26 used, composed of DMEM-HG supplemented with 1% ITS<sup>+</sup> Premix™, 100 μM  
27  
28 ascorbate-2-phosphate,  $10^{-7}$  M dexamethasone, and 10 ng/ml TGF-β1 [28]. L-  
29  
30 glutamine, antibiotic antimycotic, non-essential amino acids, and sodium pyruvate were  
31  
32 added at 1%.  
33  
34  
35

### 36 37 **Injection protocol:**

38  
39 There were seven experimental groups. Two milliliter aliquots of the cell suspension  
40  
41 were taken from the syringe using only the extension tubing, but no needle (no injection  
42  
43 controls). Aliquots were then passed through either a 22 Ga or a 25 Ga needle either  
44  
45 directly into an open collection vial at atmospheric pressure (no backpressure) or into a  
46  
47 sterile septum vial against a ~ 207 kPa (30 PSI, low backpressure) or ~ 414 kPa (60  
48  
49 PSI, high backpressure) head. Injections were done by hand and took  $26 \pm 3$  s (mean  $\pm$   
50  
51 SD). Timing and pressures were monitored and recorded.  
52  
53  
54  
55  
56  
57  
58  
59  
60  
61  
62  
63  
64  
65

1  
2  
3  
4 **Live/dead assay:**  
5

6  
7 Round glass coverslips were cleaned in a 68% nitric acid bath for 1 hour, repeated  
8  
9 once, rinsed extensively in diH<sub>2</sub>O and autoclaved. Following syringing, 4-6 replicate  
10  
11 aliquots from each treatment condition were plated at 23,000 cells/well onto the  
12  
13 coverslips in 24-well plates. 24 and 48 hours later, live dead assays were performed  
14  
15 following the manufacturers protocols (L-3224, Molecular Probes/Invitrogen). Stock  
16  
17 solutions (Calcein AM, 4 M in DMSO, ethidium homodimer, 2 mM in 25% DMSO in H<sub>2</sub>O)  
18  
19 were diluted 1:4000 in sterile Tyrode's solution. These dilutions had previously been  
20  
21 found to work well with human MSCs. The coverslips were covered with 500 µl of the  
22  
23 staining mixture for 30 minutes, after which the cover slips were wet-mounted and  
24  
25 photographed immediately at 5 × by fluorescent microscopy. Live (green cytoplasm)  
26  
27 and dead (red nuclei) cells were counted on 3-5 random fields, using ImageJ. Results  
28  
29 were expressed as percent of total cell number which stained positive with ethidium  
30  
31 homodimer.  
32  
33  
34  
35  
36  
37  
38

39 **Chondrogenic medium and aggregate culture:**  
40

41  
42 Microplate chondrogenic aggregate cultures were prepared using the remainder of the  
43  
44 cells.[29] Briefly, the cells were resuspended in chondrogenic medium (see above) at  
45  
46  $1.25 \times 10^6$  cells per ml, and 200 µl of cell suspension were then pipetted into each well  
47  
48 of an autoclaved 96-well, V-bottom, 300 µl polypropylene microplate. The plates were  
49  
50 centrifuged for 5 minutes at 500 × g and then placed in a cell culture incubator (37 °C,  
51  
52 humidified atmosphere of 95% air and 5% CO<sub>2</sub>). Twenty-four hours later, the newly  
53  
54 formed aggregates were released from the bottom of the wells to ensure that they float  
55  
56  
57  
58  
59 freely by pipetting a small volume of the medium with an 8-channel pipette. The  
60  
61  
62  
63  
64  
65

1  
2  
3  
4 chondrogenic medium was replaced every three days.

5  
6  
7 At 21 days, the aggregates were harvested, formalin-fixed, and paraffin-embedded as  
8  
9 described previously. Seven micrometer sections were stained for proteoglycan content  
10  
11 using Toluidine Blue-O. All sections (several from each aggregate) were imaged in a  
12  
13 single session in bright-field using a Leica DM-LB2 microscope and a Spot-RT camera.  
14  
15 Quantitative image analysis was performed on the resulting 8-bit per channel RGB tiff  
16  
17 images. We used ImageJ with the “Threshold Color” plugin as a band pass filter in  
18  
19 hue/saturation/brightness (HSB) mode, with a pass band of 165-255 set in the Hue  
20  
21 channel. [30] This identified the cross-sectional area of the aggregates that stained  
22  
23 metachromatically (**Fig. 1B, C, & D**), which was expressed relative to the total cross-  
24  
25 sectional area (**Fig. 1E**) of the section.  
26  
27  
28  
29  
30

### 31 32 **Modeling:**

33  
34 We used computational modeling to determine peak shear forces on the cells at the  
35  
36 transition of the syringe hub to the needle bore using a Comsol Multiphysics model. To  
37  
38 this end, molds were made of the needle hub using poly(dimethyl siloxane) (**Fig. 2**). The  
39  
40 molds were carefully measured and the dimensions used for the model.  
41  
42  
43

44  
45 We solved axi-symmetric Navier-Stokes equations in the transition region (**Fig. 3**). The  
46  
47 transition region is where the cells are expected to encounter maximum shear forces in  
48  
49 the entire system; it corresponds to the region where the conical body connects to the  
50  
51 cylindrical needle (**Fig. 2 (arrow) and 3**). Viscosity correction for cell suspensions was  
52  
53 modeled using the Einstein’s suspensions model; for the volume fraction corresponding  
54  
55 to the cell density used in the experiments, the cells had very little impact (<0.1%) on  
56  
57 the viscosity (1.001 mPa-s) of the fluid. The density of the fluid was set to 1000 kg/m<sup>3</sup>.  
58  
59  
60  
61  
62  
63  
64  
65

1  
2  
3  
4 Boundary conditions included: no slip conditions at the solid walls, inlet average velocity  
5 was specified based on the flow rate, and the outlet pressure value was specified based  
6  
7 on the measurements. Meshing was carried out to obtain extrafine meshing near the  
8  
9 walls and the transition region where the changes were expected to be dramatic. The  
10  
11 model was solved under steady-state conditions to obtain velocity and shear rate  
12  
13 profiles. Post-processing of the data was carried out to obtain shear stress profiles in  
14  
15 the system.  
16  
17  
18  
19  
20  
21

## 22 **Software packages**

23  
24 Software packages used for data acquisition and analysis include Excel (Microsoft,  
25 Redmond, WA), ImageJ [30], SPOT-RT software (Diagnostic Instruments, Sterling  
26 Heights, Michigan), Comsol Multiphysics (Comsol, Inc., Burlington, MA) and Sigmaplot /  
27  
28 Sigmastat (Systat Software, San Jose, CA), and SAS Version 9.3 (Sas Institute, Inc.,  
29  
30 Cary, NC).  
31  
32  
33  
34  
35  
36  
37

## 38 **Results**

### 41 **Modeling:**

42  
43 Velocity profiles in the system indicate that the peak values occurred along the axis of  
44  
45 the needle with values as high as 2.5 m/s (**Fig. 3A**). Despite these large values, the  
46  
47 maximum Reynolds number was about 12 in the needled groups indicating laminar flow  
48  
49 situations in the system (**Fig. 3**). Pressure profiles in the system indicate that the  
50  
51 pressure drop across the model section was around 8000 Pa. Shear rate profiles  
52  
53 showed that peak wall shear stress values occurred in the transition region (**Fig. 3B**)  
54  
55 and, for the conditions used in the experiments, they ranged from 143-247 Pa. Dwell  
56  
57  
58  
59  
60  
61  
62  
63  
64  
65

1  
2  
3  
4 time in the transition region was  $\ll 1$  sec.  
5  
6

### 7 **Cell-based experiments:**

8  
9  
10 All manipulations were accomplished under sterile conditions; there were no  
11  
12 experimental losses due to contamination.  
13  
14

### 15 **Cell viability:**

16  
17  
18 There were almost no (1-5 per 5 $\times$  field) non-attached cells in all groups, either at 24 or  
19  
20 48 hours, suggesting that the live-dead assay on cover-slip attached cells would be  
21  
22 representative of the total population. On average, 1500 cells were counted per group  
23  
24 for each day. Results of the live-dead assays are shown in **Fig. 4** for all groups at 24  
25  
26 and 48 hours after the injection procedure. With a few exceptions, the percentage of  
27  
28 ethidium-positive cells was under 10%, and in general (10 out of 14 conditions) the  
29  
30 percentage of dead cells was higher at 48 hours than at 24. However, the time effect  
31  
32 was not significant in the ANOVA analysis, and both are fairly typical of passaged MSC  
33  
34 in our hands.  
35  
36  
37  
38  
39  
40

41 For statistical analysis, the weighted mean and standard error of the proportion of dead  
42  
43 cells for each slide was calculated using multiple readings from the same slide using a  
44  
45 random-effects model used for meta-analysis [31]. The data were analyzed using a  
46  
47 weighted 3-way ANOVA, including main effects for condition (the seven combinations of  
48  
49 gauge/pressure), time (24 vs. 48 hours), and cell number (2 or 4 M cells/ml), where  
50  
51 weights were the inverses of the squared estimated standard errors of the estimated  
52  
53 percentages for each slide. Use of a main-effects only ANOVA was justified since the 2-  
54  
55 way interactions were all non-significant (all p-values  $\geq 0.45$ ). The main effect of time  
56  
57  
58  
59  
60  
61  
62  
63  
64  
65

1  
2  
3  
4 was not significant ( $p = 0.66$ ), whereas main effects for cell concentration ( $p = 0.018$ )  
5  
6 and condition ( $p = 0.015$ ) were significant. The estimated percentage of dead cells was  
7  
8 higher when the concentration was 4 M/ml as compared to 2 M/ml (mean difference =  
9  
10 0.020, 95% CI (0.004, 0.035). Pairwise comparisons of the 7 conditions correcting for  
11  
12 multiple testing using the Tukey-Kramer method found that the 22 gauge needle – low  
13  
14 backpressure condition had higher cell death as compared to both the 25 gauge needle-  
15  
16 Low and the 25 gauge needle no backpressure conditions. No other differences  
17  
18 reached statistical significance, although confidence intervals indicated that some of the  
19  
20 conditions could differ by as much as 0.10 in the proportion of dead cells. (**Fig. 4, Table**  
21  
22  
23  
24  
25  
26 **2)**

### 30 **Aggregate culture:**

31  
32 Within 24 hours of seeding the microwell plates, cells from all groups formed  
33  
34 aggregates normally. After three weeks in aggregate culture, the cells had undergone  
35  
36 chondrogenic differentiation in all cases, with morphological changes consistent with  
37  
38 previously published aggregate culture experiments, including the expression of a  
39  
40 proteoglycan (PG)-rich ECM. This suggests that none of the injection regimes had a  
41  
42 deleterious effect on the subsequent differentiation potential of the cells. Interestingly,  
43  
44 the relative metachromatic area of Toluidine blue O stained sections, an indication of  
45  
46 PG-content, was lower on the cells ( $57.3 \pm 19\%$  for the 2M cells/ml group and  $73.6 \pm$   
47  
48  $16\%$  for the 4M cells/ml group) which had not been passed through the needle  
49  
50 compared to cells which had been passed through the needle (100% in all pellets  
51  
52 examined).  
53  
54  
55  
56  
57  
58  
59  
60  
61  
62  
63  
64  
65

## Discussion

Cell therapies may be enhanced through interventional radiology. Image guided needle or catheter procedures in this setting potentially offer the advantages of a minimally invasive approach and improved efficacy through directed delivery. [25, 32, 33] When cells are handled, though, they are subjected to various forces. Key types of flow-induced forces include normal (pressure) and shear forces. It has been shown that the cells can withstand large amounts of normal forces for long durations; however, there is evidence that even brief exposure to shear forces can be deleterious to cells. In this study, we investigated the effects of injecting MSCs through spinal needles against various levels of backpressure. Our findings suggest that under the conditions tested, there was a slight but statistically significant increase in cell death in the 22 gauge needle – low backpressure treatment group vs. only two other groups, 25 gauge needle-Low and the 25 gauge needle no backpressure groups. These differences in total number of dead cells is quite small, so that we feel confident that there would be a negligible biological effect due to MSC viability in an intradisk injection scenario. This is also consistent with the lack of negative effects of the injection protocols on the function of the viable cells as determined by their chondrogenic potential in aggregate culture (see below). These findings are complemented by the results of modeling of the fluid dynamic characteristics of the system.

Live cells are routinely delivered through needles, e.g., in blood transfusions. Typically, the backpressure in such procedures is the venous pressure that is in the range of 3-8 mm Hg central or 10-12 mm Hg for peripheral circulation above atmospheric pressure.

In a previous study, Walker et al. showed that at common infusion rates (60 – 500

1  
2  
3  
4 ml/hour), through short needles of between 20 and 30 gauge, but against atmospheric  
5  
6 backpressure, rat and human MSCs were not affected in terms of viability and  
7  
8 multilineage differentiation potential. [26] That study applies to IV infusion of the cells,  
9  
10 and not necessarily to injection into solid tissue. When cells are delivered to solid  
11  
12 tissues, they can face significantly higher backpressures due to resistance to flow in the  
13  
14  
15  
16 tissue.

17  
18  
19 The feasibility of delivering MSC by high-pressure injection to the IVD using a  
20  
21 percutaneous image-guided needle has previously been shown in porcine models of  
22  
23 degenerative disc disease. [25] In that study, radiolabelled xenogenic MSC were  
24  
25 injected and imaged over time (0 and 3 days) for confirmation of delivery and  
26  
27 containment. The imaging studies were confirmed by histology, [25] however, it was not  
28  
29 clear whether the injected cells survived the procedure. In this study we show that,  
30  
31  
32 under clinically relevant conditions, resistance to flow during injection was not  
33  
34 deleterious to MSC.  
35  
36  
37

38  
39 It is well understood that excess shear can lead to cellular damage; e.g., RBC lysis after  
40  
41 passing blood through a needle is a known problem. [34] RBC lysis depends on the  
42  
43 level of shear stress and the exposure time. In general nucleated cells are considered  
44  
45 more fragile, for example with leukocyte damage being observed at 30 Pa. Both cell  
46  
47 types can withstand higher stresses if the duration of exposure is brief. Generally large-  
48  
49 bore needles and low pressures can mitigate damage, [34, 35] but spinal needles are  
50  
51 generally smaller in diameter. To understand the fluid dynamics and shear stress  
52  
53 conditions in our system, we utilized computational fluid dynamic modeling. Peak  
54  
55 stresses typically occur at flow transition conditions such as sudden diameter transitions  
56  
57  
58  
59  
60  
61  
62  
63  
64  
65



1  
2  
3  
4 in the flow conduit; in our system this is at the junction between the hub and the needle  
5  
6 **(Fig. 2 (arrow) & 3)**. Although the stresses are relatively high, at the flow velocities we  
7  
8 used, dwell time in this high-shear region would be predicted to be on the order of  
9  
10 milliseconds **(Fig. 3)**, and even then only occur at the wall of the conduit **(Fig. 3)**. Our  
11  
12 results suggest that for the conditions cells encounter in the spinal needles used in this  
13  
14 study, and using RBC criteria for MSCs, lysis would not be expected to occur.  
15  
16  
17  
18

19 The intent of the aggregate culture experiments was to determine whether there was a  
20  
21 longer term negative impact of the injection on the subsequent differentiation potential  
22  
23 of the cells. We selected chondrogenic differentiation as a general marker for the  
24  
25 differentiation potential of the cells, as this is generally the first lineage to be lost [36].  
26  
27 Rather unexpectedly, even the brief, half minute exposure to the injection procedure  
28  
29 resulted in an apparent enhanced chondrogenic differentiation. It is currently unknown  
30  
31 whether other MSC properties are similarly affected.  
32  
33  
34  
35

36 Other groups have studied the effects of shear stress on MSCs and MSC differentiation.  
37  
38 For example, Yourek et al. exposed MSCs to 24 hours of shear at 1Pa and found an  
39  
40 upregulation of osteogenic markers. Interestingly, undifferentiated MSCs were more  
41  
42 responsive to shear than partially differentiated cells [37]. In those cases, the shear  
43  
44 magnitude was lower but the duration of shear exposure was much greater, and the  
45  
46 cells were substrate attached; in such systems the contribution of shear exposure vs.  
47  
48 improved medium convection is unclear. In other studies, even brief exposure to shear  
49  
50 stresses has been shown to cause activation of certain genes in MSCs. [38] It is, thus,  
51  
52 possible that this effect could be exploited to enhance differentiation in tissue  
53  
54 engineering applications.  
55  
56  
57  
58  
59  
60  
61  
62  
63  
64  
65

1  
2  
3  
4 As interventional radiology expands and integrates with cellular medicine, multiple  
5 facets of image guided delivery that may potentially impact therapy should be  
6  
7 considered, including cellular tracking, sites of cell action, efficacy of local delivery, and  
8  
9 feasibility of needle or catheter delivery. This study investigated the effects of flow  
10  
11 induced forces introduced through needle delivery on mesenchymal stem cells in a  
12  
13 simulated model of in vitro intervertebral disc injection, indicating that the associated  
14  
15 backpressure and shear do impact the cells. Currently, injection pressure is not usually  
16  
17 recorded even when injecting into solid tissue, e.g., [39] but given the small but  
18  
19 detectable biological effects, it could be useful to document them going forward. Using  
20  
21 pressure monitoring equipment clinically would have advantages, as it has previously  
22  
23 been documented that “syringe feel” by the operator is a poor predictor of the actual  
24  
25 injection pressures. [40, 41] Further, pressure feedback can likely provide some  
26  
27 objective assessment of the quality of the tissue being injected, and can potentially  
28  
29 provide a final alert to erroneous needle tip placement. Larger in vitro and in vivo  
30  
31 studies that analyze potential effects of this impact on disc regeneration vs. other cell  
32  
33 delivery methods (surgical +/- scaffolds) are warranted.  
34  
35  
36  
37  
38  
39  
40  
41  
42  
43  
44  
45  
46  
47  
48  
49  
50  
51  
52  
53  
54  
55  
56  
57  
58  
59  
60  
61  
62  
63  
64  
65

## References

[1] Luoma K, Riihimaki H, Luukkonen R, Raininko R, Viikari-Juntura E, Lamminen A. Low back pain in relation to lumbar disc degeneration. Spine (Phila Pa 1976) 2000; 25:487-92.

[2] Madigan L, Vaccaro AR, Spector LR, Milam RA. Management of symptomatic lumbar degenerative disk disease. J Am Acad Orthop Surg 2009; 17:102-11.

[3] Boos N, Weissbach S, Rohrbach H, Weiler C, Spratt KF, Nerlich AG. Classification of age-related changes in lumbar intervertebral discs: 2002 Volvo Award in basic science. Spine (Phila Pa 1976) 2002; 27:2631-44.

[4] Frymoyer JW, Cats-Baril WL. An overview of the incidences and costs of low back pain. Orthop Clin North Am 1991; 22:263-71.

[5] Bogduk N, Karasek M. Two-year follow-up of a controlled trial of intradiscal electrothermal anuloplasty for chronic low back pain resulting from internal disc disruption. Spine J 2002; 2:343-50.

[6] Kvarstein G, Mawe L, Indahl A, et al. A randomized double-blind controlled trial of intra-annular radiofrequency thermal disc therapy--a 12-month follow-up. Pain 2009; 145:279-86.

[7] Freeman BJ, Fraser RD, Cain CM, Hall DJ, Chapple DC. A randomized, double-blind, controlled trial: intradiscal electrothermal therapy versus placebo for the treatment of chronic discogenic low back pain. Spine (Phila Pa 1976) 2005; 30:2369-77; discussion 78.

1  
2  
3  
4 [8] Hilibrand AS, Robbins M. Adjacent segment degeneration and adjacent segment  
5 disease: the consequences of spinal fusion? Spine J 2004; 4:190S-4S.  
6  
7

8  
9  
10 [9] Shuff C, An HS. Artificial disc replacement: the new solution for discogenic low back  
11 pain? Am J Orthop (Belle Mead NJ) 2005; 34:8-12.  
12  
13

14  
15  
16 [10] Yoo JU, Barthel TS, Nishimura K, et al. The chondrogenic potential of human bone-  
17 marrow-derived mesenchymal progenitor cells. J Bone Joint Surg (Am) 1998; 80:1745-  
18 57.  
19  
20  
21

22  
23  
24 [11] Richardson SM, Hoyland JA, Mobasheri R, Csaki C, Shakibaei M, Mobasheri A.  
25 Mesenchymal stem cells in regenerative medicine: opportunities and challenges for  
26 articular cartilage and intervertebral disc tissue engineering. J Cell Physiol 2010;  
27 222:23-32.  
28  
29  
30

31  
32  
33 [12] Henriksson HB, Svanvik T, Jonsson M, et al. Transplantation of human  
34 mesenchymal stems cells into intervertebral discs in a xenogeneic porcine model. Spine  
35 (Phila Pa 1976) 2009; 34:141-8.  
36  
37  
38

39  
40  
41 [13] Yang H, Wu J, Liu J, et al. Transplanted mesenchymal stem cells with pure  
42 fibrinous gelatin-transforming growth factor-beta1 decrease rabbit intervertebral disc  
43 degeneration. Spine J 2010; 10:802-10.  
44  
45  
46

47  
48  
49 [14] Solchaga LA, Welter JF, Lennon DP, Caplan AI. Generation of pluripotent stem  
50 cells and their differentiation to the chondrocytic phenotype. Methods Mol Med 2004;  
51 100:53-68.  
52  
53  
54  
55  
56  
57  
58  
59  
60  
61  
62  
63  
64  
65

1  
2  
3  
4 [15] Solchaga LA, Penick K, Goldberg VM, Caplan AI, Welter JF. Fibroblast growth  
5 factor-2 enhances proliferation and delays loss of chondrogenic potential in human adult  
6 bone-marrow-derived mesenchymal stem cells. Tissue engineering Part A 2010;  
7 16:1009-19.  
8  
9

10  
11  
12  
13  
14  
15 [16] Sobajima S, Vadala G, Shimer A, Kim JS, Gilbertson LG, Kang JD. Feasibility of a  
16 stem cell therapy for intervertebral disc degeneration. Spine J 2008; 8:888-96.  
17  
18  
19

20  
21 [17] Sakai D, Mochida J, Iwashina T, et al. Differentiation of mesenchymal stem cells  
22 transplanted to a rabbit degenerative disc model: potential and limitations for stem cell  
23 therapy in disc regeneration. Spine (Phila Pa 1976) 2005; 30:2379-87.  
24  
25  
26

27  
28  
29 [18] Crevensten G, Walsh AJ, Ananthakrishnan D, et al. Intervertebral disc cell therapy  
30 for regeneration: mesenchymal stem cell implantation in rat intervertebral discs. Ann  
31 Biomed Eng 2004; 32:430-4.  
32  
33  
34

35  
36  
37 [19] Zhang YG, Guo X, Xu P, Kang LL, Li J. Bone mesenchymal stem cells transplanted  
38 into rabbit intervertebral discs can increase proteoglycans. Clin Orthop Relat Res  
39 2005:219-26.  
40  
41  
42  
43

44  
45  
46 [20] Bendtsen M, Bunker CE, Zou X, Foldager C, Jorgensen HS. Autologous stem cell  
47 therapy maintains vertebral blood flow and contrast diffusion through the endplate in  
48 experimental intervertebral disc degeneration. Spine (Phila Pa 1976) 2011; 36:E373-9.  
49  
50  
51  
52

53  
54 [21] Serigano K, Sakai D, Hiyama A, Tamura F, Tanaka M, Mochida J. Effect of cell  
55 number on mesenchymal stem cell transplantation in a canine disc degeneration model.  
56 J Orthop Res 2010; 28:1267-75.  
57  
58  
59  
60  
61  
62  
63  
64  
65

1  
2  
3  
4 [22] Orozco L, Soler R, Morera C, Alberca M, Sanchez A, Garcia-Sancho J.  
5  
6 Intervertebral disc repair by autologous mesenchymal bone marrow cells: a pilot study.  
7  
8 Transplantation 2011; 92:822-8.  
9

10  
11  
12 [23] Yoshikawa T, Ueda Y, Miyazaki K, Koizumi M, Takakura Y. Disc regeneration  
13  
14 therapy using marrow mesenchymal cell transplantation: a report of two case studies.  
15  
16 Spine (Phila Pa 1976) 2010; 35:E475-80.  
17  
18

19  
20  
21 [24] Mesoblast I. United States FDA clears Mesoblast phase 2 trial to treat degenerative  
22  
23 disc disease. Melbourne, Australia, 2011.  
24  
25

26  
27 [25] Prologo JD, Pirasteh A, Tenley N, et al. Percutaneous image-guided delivery for the  
28  
29 transplantation of mesenchymal stem cells in the setting of degenerated intervertebral  
30  
31 discs. J Vasc Interv Radiol 2012; 23:1084-8 e6.  
32  
33

34  
35 [26] Walker PA, Jimenez F, Gerber MH, et al. Effect of needle diameter and flow rate on  
36  
37 rat and human mesenchymal stromal cell characterization and viability. Tissue Eng Part  
38  
39 C, Meth 2010; 16:989-97.  
40  
41

42  
43 [27] Lennon DP, Haynesworth SE, Bruder SP, Jaiswal N, Caplan AI. Human and animal  
44  
45 mesenchymal progenitor cells from bone marrow: Identification of serum for optimal  
46  
47 selection and proliferation. In Vitro Cell Dev Biol 1996; 32:602-11.  
48  
49

50  
51  
52 [28] Johnstone B, Hering TM, Caplan AI, Goldberg VM, Yoo JU. In vitro chondrogenesis  
53  
54 of bone marrow-derived mesenchymal progenitor cells. Exp Cell Res 1998; 238:265-72.  
55  
56

57  
58 [29] Penick KJ, Solchaga LA, Welter JF. High-throughput aggregate culture system to  
59  
60  
61  
62  
63  
64  
65

1  
2  
3  
4 assess the chondrogenic potential of mesenchymal stem cells. *Biotechniques* 2005;  
5  
6 39:687-91.  
7

8  
9  
10 [30] Schneider CA, Rasband WS, Eliceiri KW. NIH Image to ImageJ: 25 years of image  
11  
12 analysis. *Nat Methods* 2012; 9:671-5.  
13

14  
15  
16 [31] DerSimonian R, Laird N. Meta-analysis in clinical trials. *Control Clin Trials* 1986;  
17  
18 7:177-88.  
19

20  
21  
22 [32] Nikolic B, Faintuch S, Goldberg SN, Kuo MD, Cardella JF. Stem cell therapy: a  
23  
24 primer for interventionalists and imagers. *Journal of vascular and interventional*  
25  
26 *radiology : JVIR* 2009; 20:999-1012.  
27

28  
29  
30 [33] Avritscher R, Abdelsalam ME, Javadi S, et al. Percutaneous Intraportal Application  
31  
32 of Adipose Tissue-derived Mesenchymal Stem Cells Using a Balloon Occlusion  
33  
34 Catheter in a Porcine Model of Liver Fibrosis. *Journal of vascular and interventional*  
35  
36 *radiology : JVIR* 2013; 24:1871-8.  
37

38  
39  
40 [34] Miller MA, Schlueter AJ. Transfusions via hand-held syringes and small-gauge  
41  
42 needles as risk factors for hyperkalemia. *Transfusion (Paris)* 2004; 44:373-81.  
43  
44

45  
46  
47 [35] Frelich R, Ellis MH. The effect of external pressure, catheter gauge, and storage  
48  
49 time on hemolysis in RBC transfusion. *Transfusion (Paris)* 2001; 41:799-802.  
50

51  
52  
53 [36] Pittenger MF, Mbalaviele G, Black M, Mosca JD, Marshak DR. Mesenchymal stem  
54  
55 cells. In: Koller MR, Palsson BO, Masters JRW, eds. *Primary mesenchymal cells*.  
56  
57 Dordrecht; Boston: Kluwer Academic Publishers, 2001; p. 189-207.  
58  
59  
60  
61  
62  
63  
64  
65

1  
2  
3  
4 [37] Yourek G, McCormick SM, Mao JJ, Reilly GC. Shear stress induces osteogenic  
5  
6 differentiation of human mesenchymal stem cells. *Regenerative medicine* 2010; 5:713-  
7  
8 24.  
9

10  
11  
12 [38] Glossop JR, Cartmell SH. Effect of fluid flow-induced shear stress on human  
13  
14 mesenchymal stem cells: differential gene expression of IL1B and MAP3K8 in MAPK  
15  
16 signaling. *Gene expression patterns : GEP* 2009; 9:381-8.  
17  
18  
19

20  
21 [39] Berry MF, Engler AJ, Woo YJ, et al. Mesenchymal stem cell injection after  
22  
23 myocardial infarction improves myocardial compliance. *Am J Physiol Heart Circ Physiol*  
24  
25 2006; 290:H2196-203.  
26  
27

28  
29 [40] Theron PS, Mackay Z, Gonzalez JG, Donaldson N, Blanco R. An animal model of  
30  
31 "syringe feel" during peripheral nerve block. *Reg Anesth Pain Med* 2009; 34:330-2.  
32  
33

34  
35 [41] Claudio R, Hadzic A, Shih H, et al. Injection pressures by anesthesiologists during  
36  
37 simulated peripheral nerve block. *Reg Anesth Pain Med* 2004; 29:201-5.  
38  
39  
40  
41  
42  
43  
44  
45  
46  
47  
48  
49  
50  
51  
52  
53  
54  
55  
56  
57  
58  
59  
60  
61  
62  
63  
64  
65



1  
2  
3  
4 **Table Legends**  
5

6  
7 **Table 1:** Injection conditions used. No backpressure signifies injection against  
8 atmospheric pressure. Low and high were against 30 and 60 PSI (207 & 414 kPa,  
9 respectively) above atmospheric  
10  
11

12  
13  
14 **Table 2.** Differences in proportion of dead cells, estimated from a weighted analysis of  
15 variance. Because 2-way interactions with time (or among any other two factors) were  
16 not significant, when comparing conditions we averaged over the four  
17 time/concentration groups in each condition. Confidence intervals are simultaneous  
18 95% Tukey-Kramer confidence intervals. Asterisks denote differences significant at the  
19 0.05 level using the Tukey-Kramer multiple comparisons adjustment.  
20  
21  
22  
23  
24  
25  
26  
27  
28  
29  
30  
31  
32  
33  
34  
35  
36  
37  
38  
39  
40  
41  
42  
43  
44  
45  
46  
47  
48  
49  
50  
51  
52  
53  
54  
55  
56  
57  
58  
59  
60  
61  
62  
63  
64  
65

1  
2  
3  
4 **Figure Legends:**  
5

6  
7 **Fig. 1:** Schematic of the image analysis approach used to measure metachromatically-  
8 stained cross-sectional area fraction in chondrogenic aggregates. **A:** original image  
9 mosaic. **B:** segmentation. **C:** binary transformation of **B.** **D:** area measured. **E:** cross  
10 sectional area of the whole section. Metachromatic fraction was defined as the area in **D**  
11 divided by the area in **E.**  
12  
13  
14  
15  
16  
17  
18

19 **Fig. 2:** Silicone rubber mold of the interior of the needle hub. Arrow points to the  
20 transition from the hub to the needle. This mold was then measured to generate the  
21 geometry of the Comsol model  
22  
23  
24  
25  
26

27 **Fig. 3:** Comsol Model output. **A) Velocity Profile:** Velocity profile (m/sec) in the  
28 transition region between the hub and the needle. The insert (red rectangular box)  
29 shows the transition region which is expanded to show changes in velocity profiles.  
30  
31  
32  
33  
34  
35  
36  
37  
38  
39  
40  
41  
42  
43  
44  
45  
46  
47  
48  
49  
50  
51  
52  
53  
54  
55  
56  
57  
58  
59  
60  
61  
62  
63  
64  
65

Except for the transition region, the velocity profile is constant in the axial direction. **B)**  
**Shear Rate:** Shear rate profile (1/sec) in the transition region between the hub and the  
needle. The insert (red rectangular box) shows the transition region which is expanded  
to show changes in shear rates. Only in the 'neck' surface of the transition region, the  
shear rates are high. Note that the shear stress is proportional to shear rate for  
Newtonian fluids.

**Fig. 4:** Percent dead cells at 24 and 48 hours for each condition. See **Table 1** for group  
designations, **Table 2** for statistical analysis results.

Figure 1  
[Click here to download high resolution image](#)

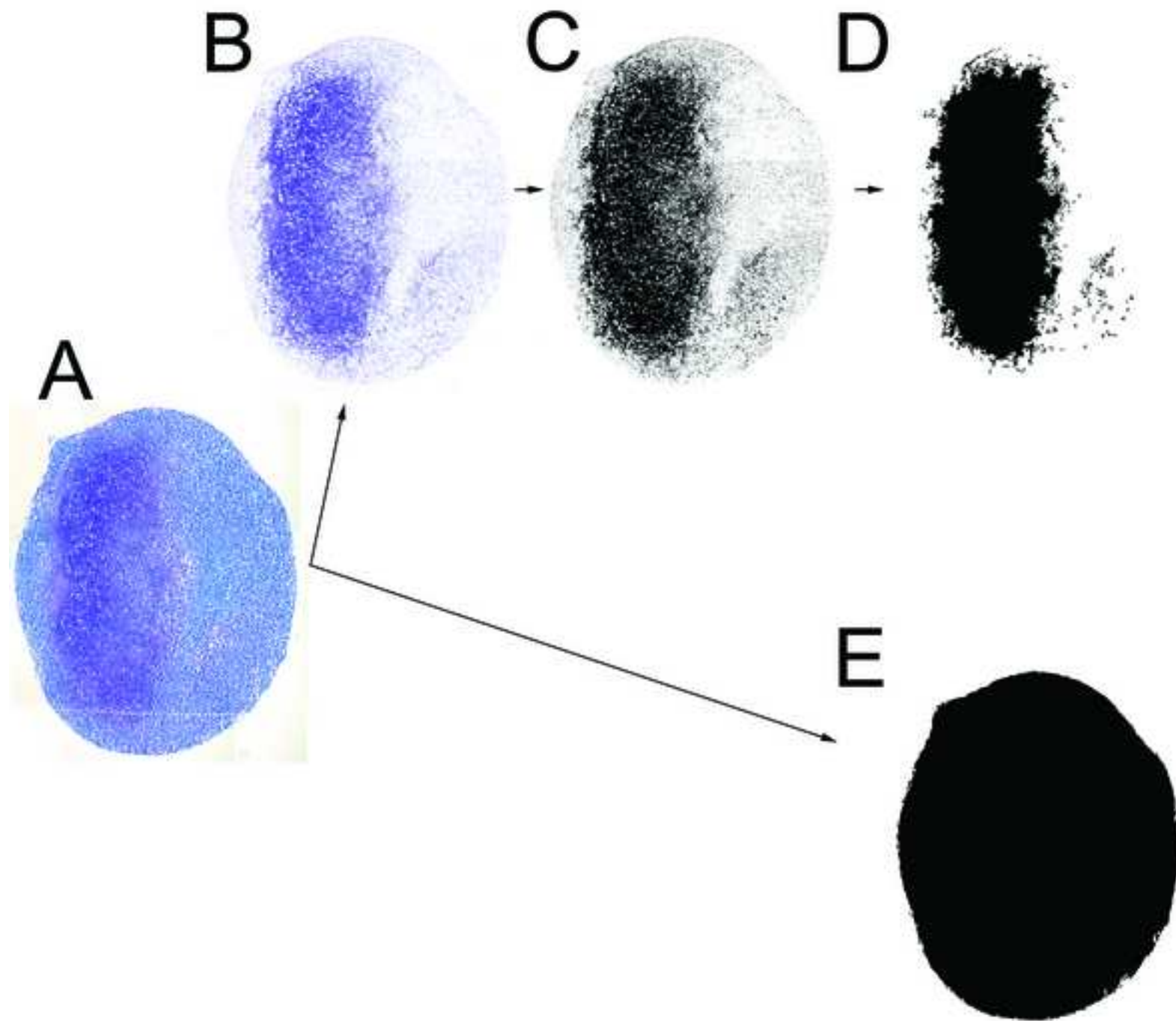


Figure 2  
[Click here to download high resolution image](#)

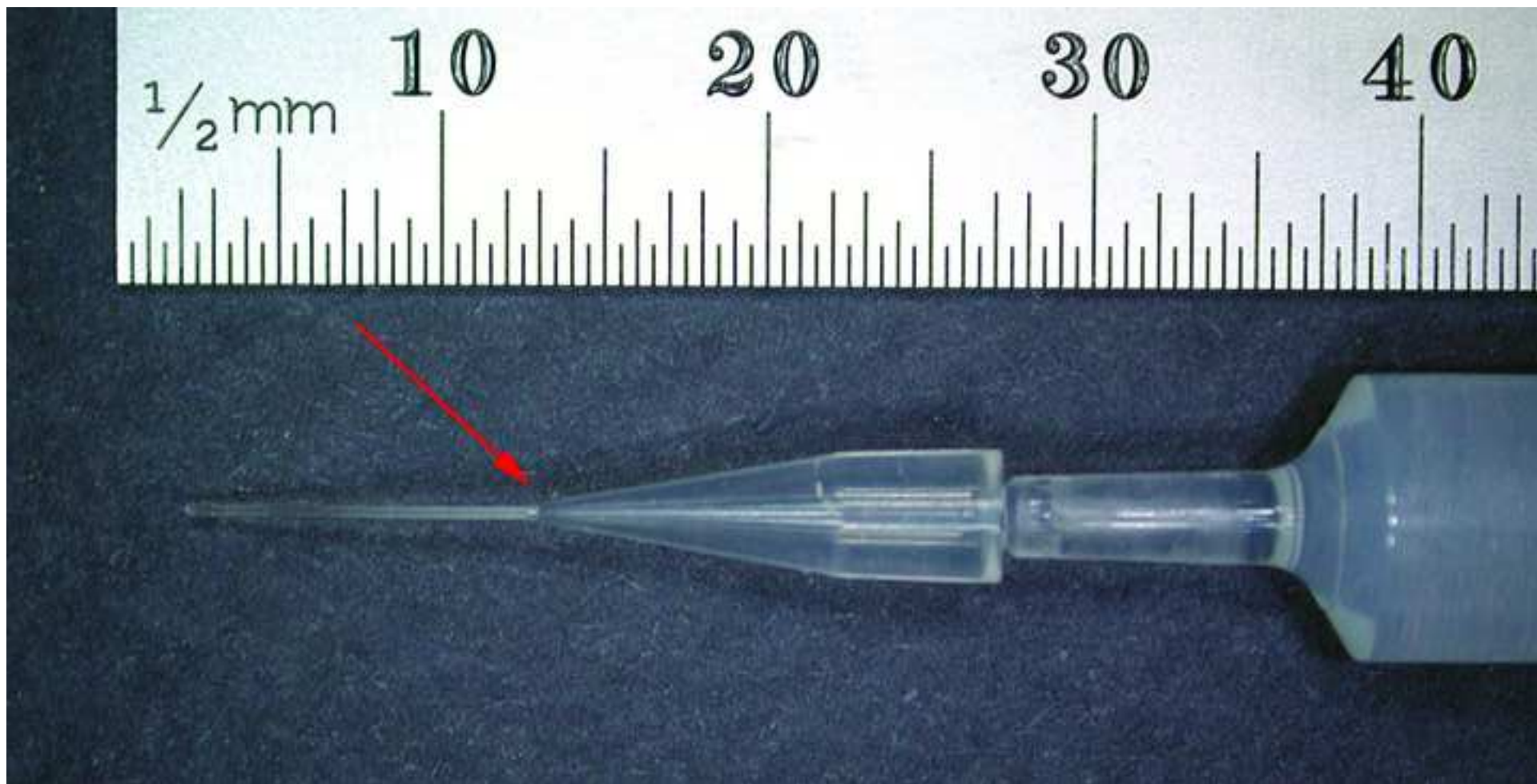


Figure 3  
[Click here to download high resolution image](#)

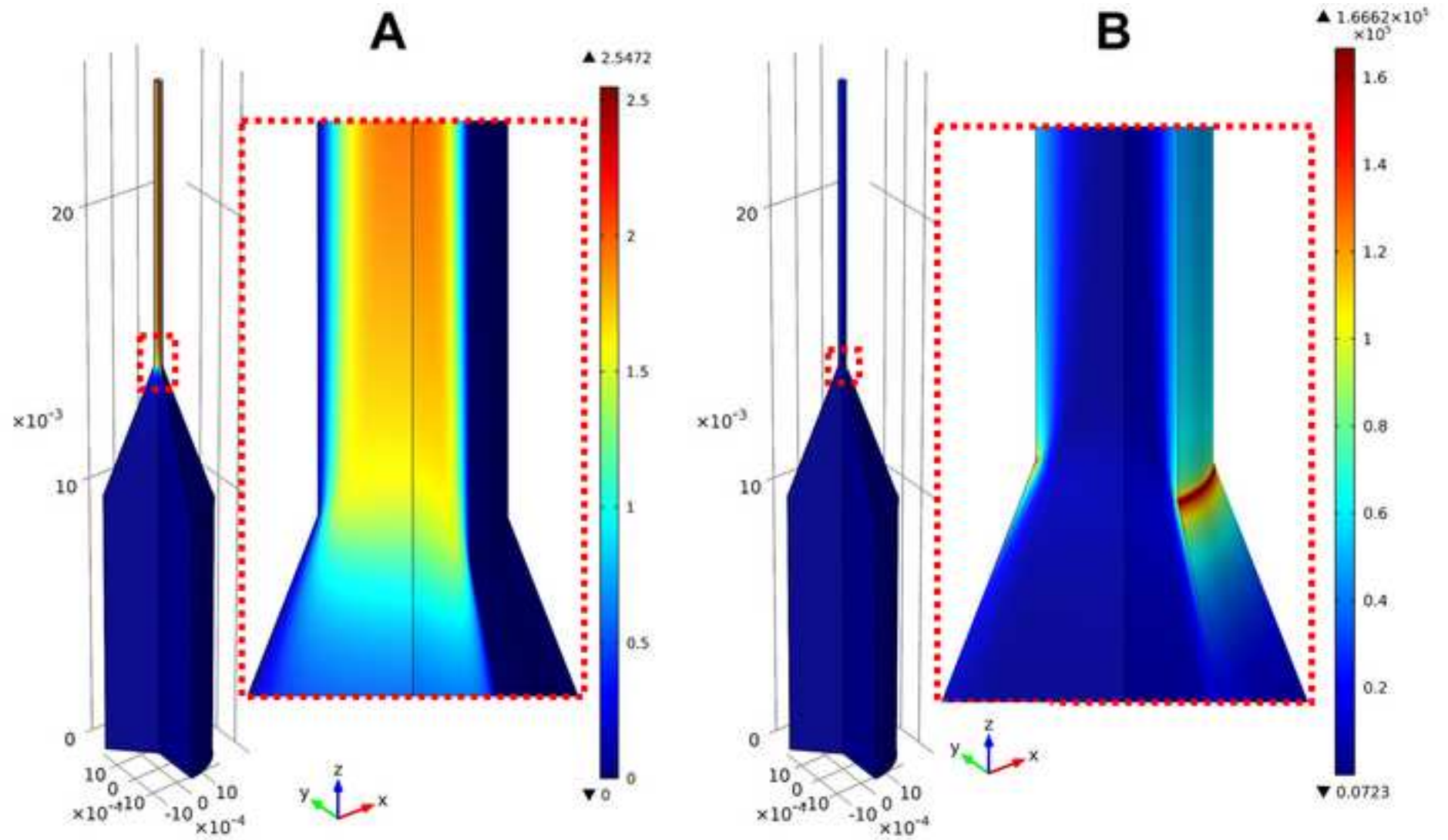
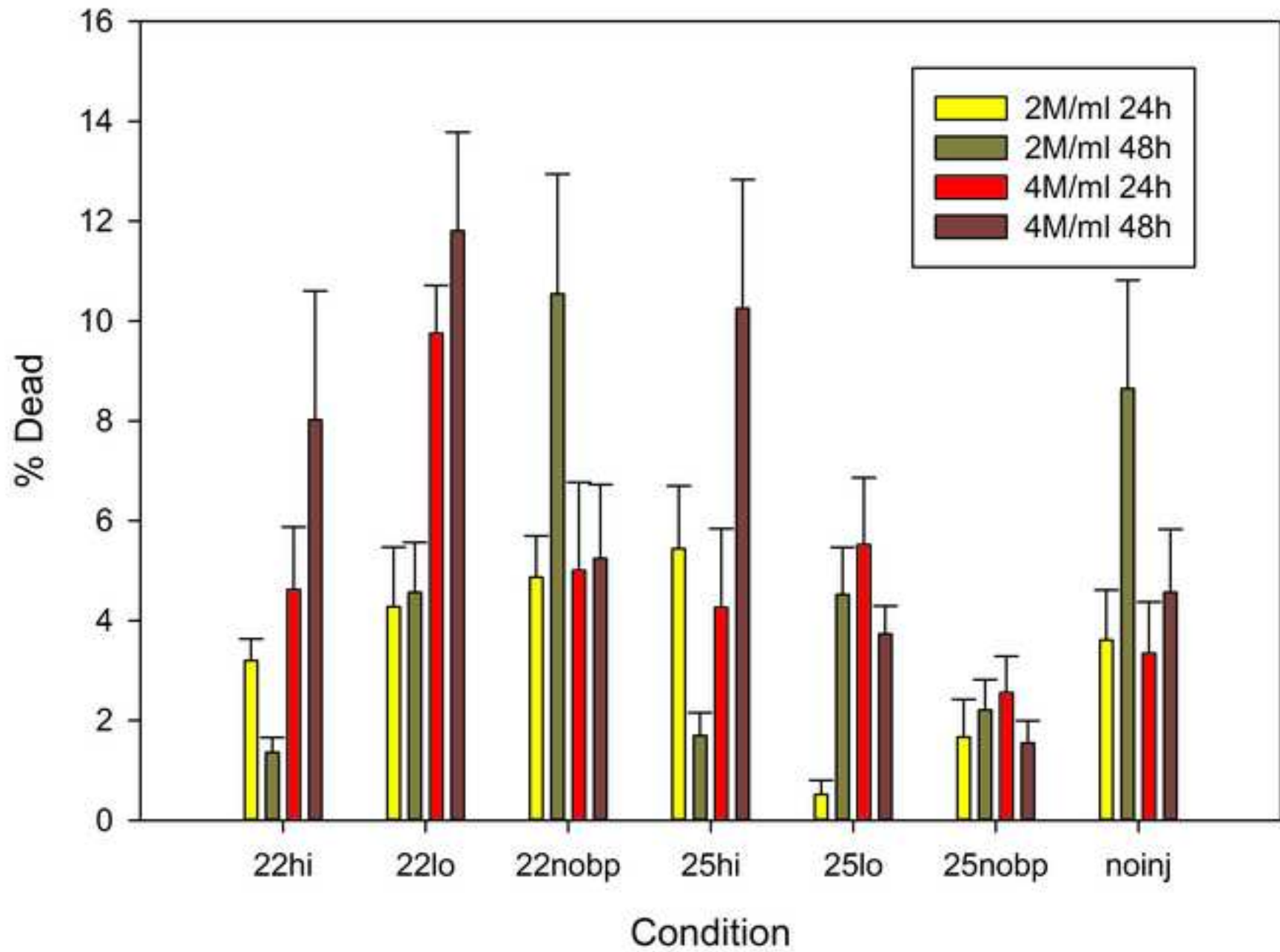


Figure 4  
[Click here to download high resolution image](#)



**Table 1**

	Needle	Backpressure	Designation
1	No	No	noinj
2	22g	No	22nobp
3	22g	Low	22lo
4	22g	High	22hi
5	25g	No	25nobp
6	25g	Low	25lo
7	25g	High	25hi

**Table 1:** Injection conditions used. No backpressure signifies injection against atmospheric pressure. Low and high were against 30 and 60 PSI (207 & 414 kPa, respectively) above atmospheric

Table 2

Comparison	Mean Difference	95% CI	
22hi - 22lo	-0.040	(-0.087, 0.006)	
22hi - 22nobp	-0.026	(-0.077, 0.025)	
22hi - 25hi	-0.003	(-0.038, 0.031)	
22hi - 25lo	0.010	(-0.016, 0.037)	
22hi - 25nobp	0.013	(-0.018, 0.044)	
22hi - noinj	-0.009	(-0.058, 0.040)	
22lo - 22nobp	0.014	(-0.048, 0.077)	
22lo - 25hi	0.037	(-0.016, 0.090)	
22lo - 25lo	0.051	(0.005, 0.096)	*
22lo - 25nobp	0.053	(0.006, 0.100)	*
22lo - noinj	0.031	(-0.029, 0.091)	
22nobp - 25hi	0.023	(-0.034, 0.080)	
22nobp - 25lo	0.036	(-0.013, 0.086)	
22nobp - 25nobp	0.039	(-0.013, 0.091)	
22nobp - noinj	0.017	(-0.047, 0.081)	
25hi - 25lo	0.014	(-0.023, 0.051)	
25hi - 25nobp	0.016	(-0.023, 0.056)	
25hi - noinj	-0.006	(-0.061, 0.050)	
25lo - 25nobp	0.003	(-0.027, 0.033)	



25lo – noinj	-0.019	(-0.067, 0.028)
25nobp – noinj	-0.022	(-0.071, 0.027)

**Table 2.** Differences in proportion of dead cells, estimated from a weighted analysis of variance. Because 2-way interactions with time (or among any other two factors) were not significant, when comparing conditions we averaged over the four time/concentration groups in each condition. Confidence intervals are simultaneous 95% Tukey-Kramer confidence intervals. Asterisks denote differences significant at the 0.05 level using the Tukey-Kramer multiple comparisons adjustment.